

## The Evaluation of Drag and Lift Force of Groove Cylinder in Wind Tunnel

Open  
Access

Wan Mohamad Aiman Wan Yahaya<sup>1,\*</sup>, Syahrullail Samion<sup>1</sup>, Fazila Mohd Zawawi<sup>1</sup>, Mohd Nor Musa<sup>1</sup>, Muhammad Naim Aiman Najurudeen<sup>1</sup>

<sup>1</sup> School of Mechanical Engineering, Faculty of Engineering, Universiti Teknologi Malaysia, 81310 UTM Skudai, Johor, Malaysia

### ARTICLE INFO

### ABSTRACT

#### Article history:

Received 16 October 2019

Received in revised form 7 January 2020

Accepted 7 January 2020

Available online 30 March 2020

Cylindrical structures subjected to flow are widely used in marine and offshore engineering and in structural applications. It has been shown that circular cylinder surface modifications can affect the separation point to move backward on the cylinder surface. Thus, reducing the drag coefficient. Flow past a circular cylinder with smooth, half and full rectangular, grooved surfaces (roughness coefficient  $k/D=0.04$ ) were investigated in a low-speed open ended wind tunnel. The outer diameters ( $D$ ) of the cylinders were 50mm and the depths ( $k$ ) of the grooves were 2mm. The Reynold's number ranged from  $1.65 \times 10^4$  to  $1.13 \times 10^5$ . The drag and lift coefficients of the cylinders were measured using a three-component balance. The wake flow patterns of the cylinders were observed using a smoke visualization technique. The results show that the full grooves and half grooves facing the flow produced a lower drag than a smooth cylinder with a half groove located at the leeside of the flow. The full grooved cylinder showed a drag reduction of 55% at  $Re=1 \times 10^5$ . The presence of the groove on the cylinder's surface tripped the boundary layer and showed a smaller and narrower wake than a smooth cylinder.

#### Keywords:

Drag force; lift force; wind tunnel;  
aerodynamics; flow visualization

Copyright © 2020 PENERBIT AKADEMIA BARU - All rights reserved

## 1. Introduction

Flow over a circular cylinder is known to be one of the fundamental concepts of fluid mechanics. This is due to the wide application of cylindrical structures in offshore and marine engineering fields; including marine pipelines, jackets, and the jack-up and tension-leg platforms and bundles of marine risers. Circular cylinders produce large drag due to the pressure difference between upstream and downstream directions of flow [1]. Something else that can be used for marine engineering is the use of vegetable-based lubricants within their machines to prevent worse oil leaks and oil biodegradability related problems [2-6].

\* Corresponding author.

E-mail address: [wmainan91@gmail.com](mailto:wmainan91@gmail.com) (Wan Mohamad Aiman Wan Yahaya)

<https://doi.org/10.37934/arfmts.68.2.4150>

The force that a flowing fluid exerts on a body, in the flow direction, is called drag. A circular cylinder generates high mean drag and large fluctuating forces [7]. Amongst other things, the drag and lift forces depend on fluid density, the upstream velocity, the size, and the shape and orientation of the body. It is impractical to list these forces for the variety of situations available. Instead, it is more convenient to work with the appropriate dimensionless numbers that represent the drag and lift characteristics. These numbers are the drag coefficient,  $C_D$  and lift coefficient,  $C_L$ .

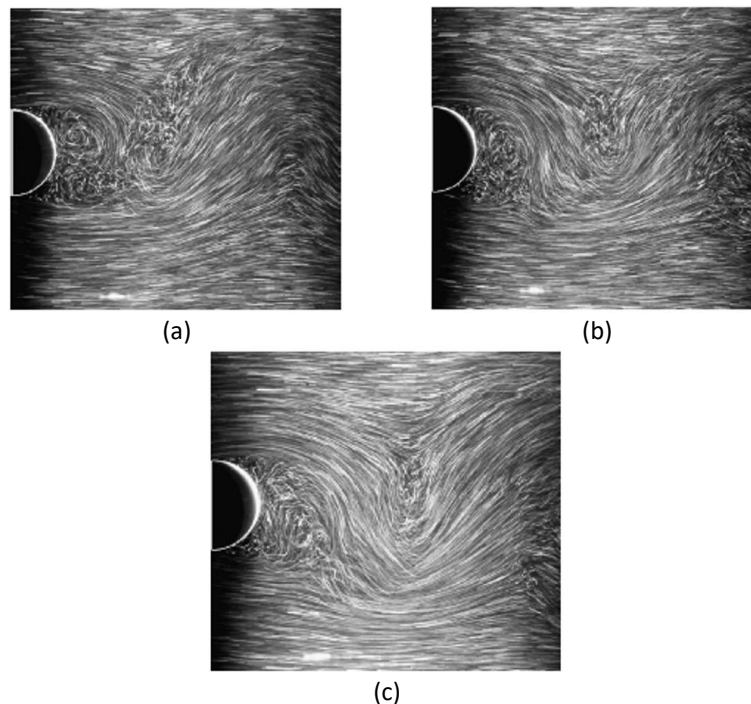


**Fig. 1.** (a) Smooth circular cylinder, (b) V-grooved cylinder and (c) U-grooved cylinder visualized flow using particle tracer method [10]

The high drag produced by circular cylinders result in finding new methods of drag reduction. Various active and passive flow control methods have been successfully implemented and tested to reduce the amount of drag or the drag coefficient [8]. Passive flow control methods require no auxiliary power or control loop. In order to reduce the amount of drag or the drag coefficient, flow control techniques are applied [9]. Flow control techniques are divided into active and passive control techniques. Active control techniques are flow control techniques that require a power input. This includes suction flow, oscillation of cylinder, synthetic jets, etc. Meanwhile, passive flow control techniques do not require a power input; but instead, normally involve cylinder surface modifications. Figure 1 shows the classification of the control techniques taken from Doreti and Dineshkumar [10].

Passive control techniques normally involve surface modifications through the addition of extra devices. However, instead of adding devices, cylinder surface texture modifications can also lead to good vortex suppression and drag reduction. Surface texture modifications include sand roughened surfaces [11-13], dimples [14,15], and grooves [16,17]. These studies show that the forces acting on a cylinder can be modified through surface modifications.

Zhuo *et al.*, [18] studied the reduction of drag and vortex induced vibration (VIV) of cylinders. According to their results, grooved and dimpled cylinders showed a smaller recirculation length than smooth cylinders. This shows that grooved and dimpled cylinders produced smaller wakes than

smooth cylinders. Another study, by Lim *et al.*, [19], used three-cylinder test models that included a smooth cylinder, a V-shaped grooved cylinder and a U-shaped grooved cylinder. The result showed that both of the grooved cylinder models produced a smaller wake width than the smooth cylinder. The wake width reduction of the U-grooved cylinder was approximately 6.4%.

This paper focuses on determining the lift,  $C_L$  and drag coefficient,  $C_D$  of a cylinder, and observing the flow separation and streamline of the cylinder. The results of three-cylinder models are then analyzed and discussed. The results are compared to previous studies conducted by various researchers.

## 2. Analysis and Experimental Set-up

### 2.1 Drag and Lift Coefficient

Drag coefficient commonly denoted as  $C_D$  is a non-dimensional quantity computed from the total pressure over the platform area and then normalized by the dynamic pressure. The drag force is the net force exerted by a fluid on a body subjected to a flow due to combined effects of wall shear and pressure forces. The part of drag due to wall shear stress,  $\tau_w$  is called skin friction drag or friction drag while the part due to pressure is known as pressure drag. Drag coefficient is defined as:

$$C_D = \frac{F_D}{\frac{1}{2}\rho V^2 S} \quad (1)$$

where

$F_D$ : Drag Force

$\rho$ : Density of air

$V$ : Velocity of air

$S$ : Projected area

Lift Coefficient is a dimensionless coefficient that relates the lift generated by a lifting body to the fluid density around the body, the fluid velocity and an associated reference area. In an airfoil, the non-dimensional quantity is a function of the Reynolds number and the angle of attack. The Reynolds number influence can be seen through the inclusion of incoming air flow density ( $\rho_\infty$ ) and its velocity ( $V_\infty$ ) terms. The lift coefficient is denoted as  $C_L$  and defined as:

$$C_L = \frac{F_L}{\frac{1}{2}\rho V^2 S} \quad (2)$$

where

$F_L$ : Lift force

### 2.2 Specimen Model

The size of cylinder used for this project is limited to the wind tunnel section size. Three cylinder models with different surface modifications were fabricated. The cylinder models were made of solid acrylic rods. The final overall diameter and the length of all the cylinders are 50mm and 190mm. A slot with a diameter of 16mm and a depth of 70mm were machined on one circular end surface of the cylinders. Figure 2 shows the cylinder with smooth surface used for this experiment.

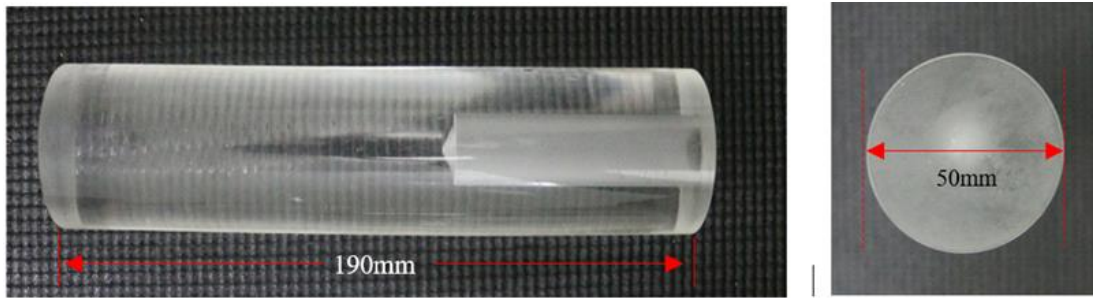


Fig. 2. The cylinder with smooth surface and its dimension

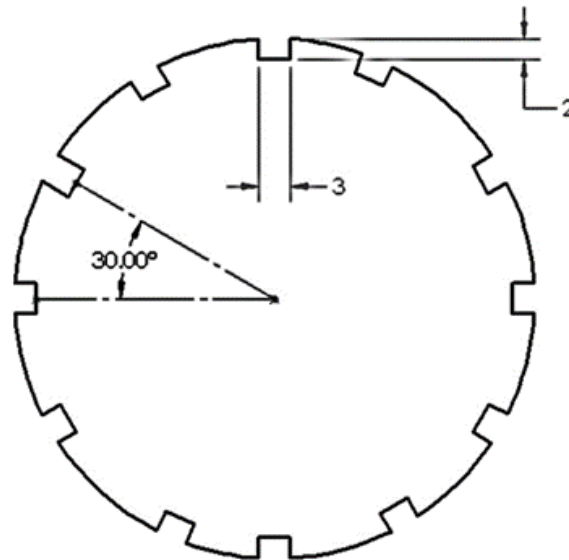


Fig. 3. Cross-sectional design of the groove cylinder

Out of three models, two of the cylinder models was designed with shallow grooves on it. One of the cylinders was partially grooved while the other was fully grooved. The grooves were machined with a longitudinal orientation type. The grooves also were equally spaced along the circle circumference. The full groove cylinder had 12 grooves covering the whole circular circumference while the half groove had 6 equally spaced groove covering only half of the circular circumference. The cross-section design of the groove cylinder is shown in Figure 3. The width ( $w$ ) and depth ( $k$ ) of the grooves were 3mm and 2mm.

### 2.3 Experimental Set-up

The experiment has been conducted by using Low Speed open end wind tunnel. A three-component balance is used to measure the drag coefficient,  $C_D$  and lift coefficient,  $C_L$  of circular cylinder object. Firstly, the cylinder test model is mounted to the supporting rod in the test section of the wind tunnel as shown in Figure 4, after the test object have been installed in the test section, the three-component balance was adjusted to ensure the angle of attack are at 0 degree. When the cylinder object is surely attached to the rod, the measured temperature and pressure values including the chord and width length of cylinder is recorded and filled into data acquisition software, the velocity is set to 5.2 m/s by turning rotated the roller switch gradually and wait for 10 second to make sure the flow is stable. The lift and drag coefficient of the cylinder models was obtained through wind tunnel testing performed at airspeed of 5.2, 8.4, 10.6, 15.4, 20.5, 25.5, 30.5 and 35.5 m/s. The

wind velocity used in this experiment are equal with Reynolds number range from  $2 \times 10^4$  to  $1.2 \times 10^5$ . Since the project is conducted in a wind tunnel, the air density is in used. Therefore, the value is of air density ( $\rho$ ) taken at temperature  $27^\circ\text{C}$  at atmospheric pressure is  $1.173\text{kg/m}^3$ . The dynamic viscosity ( $\mu$ ) is  $0.0000185\text{ kg/(m.s)}$ .



Fig. 4. Cylinder test model installed in the test section

### 3. Result and Discussion

#### 3.1 Effect of Drag Coefficient at Certain Velocity

The result obtained for the smooth cylinder are compared against the full groove cylinder. The results are compared from speed of  $5.2\text{m/s}$  to  $35.5\text{m/s}$ . The graph is presented in Figure 5, Based on the graph, both cylinders obtained a similar trend where the drag coefficient decreases corresponding to the increase in velocity. However, it could be observed that the results of both cylinders decrease drastically at velocity ranging from  $5.2\text{m/s}$  to  $15.4\text{ m/s}$ . The drag coefficient values then decrease gradually from  $15.4\text{m/s}$  up to  $35.5\text{m/s}$ . The presence of grooves on the full groove cylinder resulted to a lower drag coefficient values compared to the smooth cylinder. These results are having a same finding that reported by Zhou *et al.*, [18], where the groove cylinder values are significantly lower than those of the smooth cylinder. According to Cui *et al.*, [20], the presence of groove increases the surface roughness and this trips the boundary layer into turbulence at lower Reynolds number. Hence, the flow separation is delayed and the wake is narrowed and reducing the pressure drag considerably.

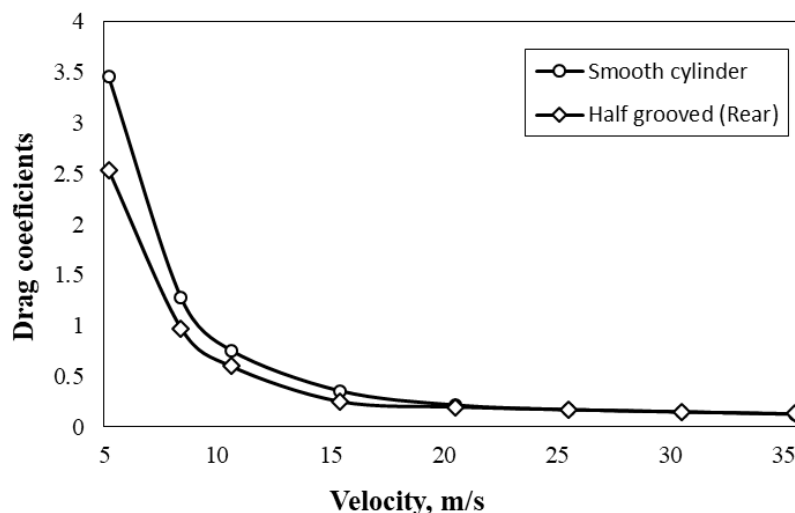


Fig. 5. Graph of Drag coefficient against velocity for smooth cylinder and full groove cylinder

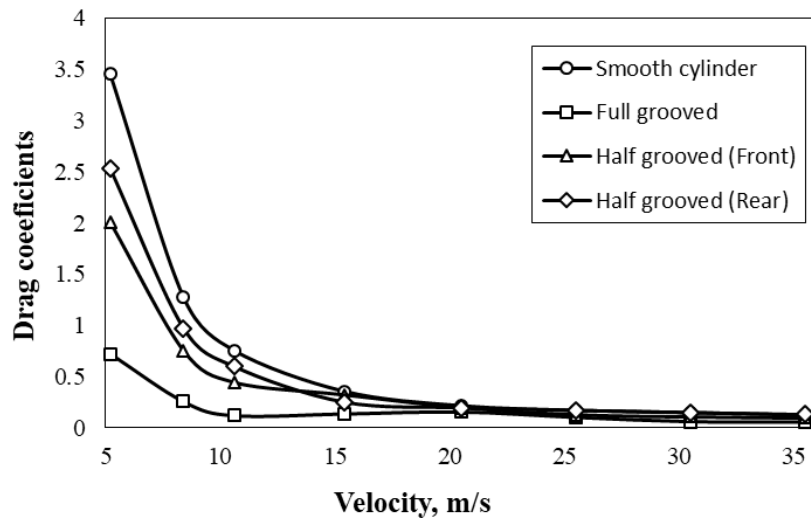


Fig. 6. Graph of Drag coefficient against velocity

The half groove cylinder was tested with two different orientations where the first one involves the groove side of the cylinder is placed towards the flow direction while for the second one the groove side is placed on the leeward side of the flow. Based on Figure 6, the drag coefficient values for all the cylinders decrease as the velocity increases. The half groove cylinder facing front recorded lower drag coefficient values followed by the rear facing half groove cylinder and then the smooth cylinder. According to Cheng *et al.*, [21], when the surface texture is located at the sheltered side, the CD are closer to or could be higher than that of a smooth cylinder.

From Figure 5 also, the drag coefficient values of the rear facing half groove cylinder are higher compared to the others. The drag coefficient of the cylinders decreases when the speed increases. It can be observed that up to 10.6 m/s the drag coefficient values decrease drastically and then start to remain relatively constant at higher velocities. Besides that, the half groove facing rear could be said inefficient in drag reduction. The test results obtained by Song *et al.*, [17] demonstrated that, by adjusting the placement of the groove, the capability of grooves on cylinder drag reduction will be further improved. The author also addresses that larger turbulence and higher Reynolds number of flows caused by grooves at the rear area may lead to lower pressure, all of which have negative effects on drag reduction.

### 3.2 Lift Coefficient

The results of lift coefficient, for all cylinder types i.e., smooth, full grooved, front half surface grooved, and rear half surface grooved, tested at eight different speeds, are plotted in Figure 7. The results obtained clearly show that lift coefficient (CL) values are considerably affected by groove pattern and groove orientation of the half grooves; with respect to incident flow, all be it in relatively small values. The graph trend indicates that the lift coefficient of the cylinders decreased with increasing velocity. However, it can be observed that the lift coefficient values fluctuate at certain speeds, such as 10.6 m/s for the full grooved cylinder and 15.4 m/s for the front facing half grooved cylinder. Zhou *et al.*, [18] stated that the lift force on the cylinder fluctuates at a certain velocity that corresponds to the periodic vortex shedding from the cylinder. Salam *et al.*, [22] stated in their book that a sphere or cylinder produces zero lift due to a top-bottom symmetry. The lift coefficient can be further increased if the cylinders are subjected to rotation.

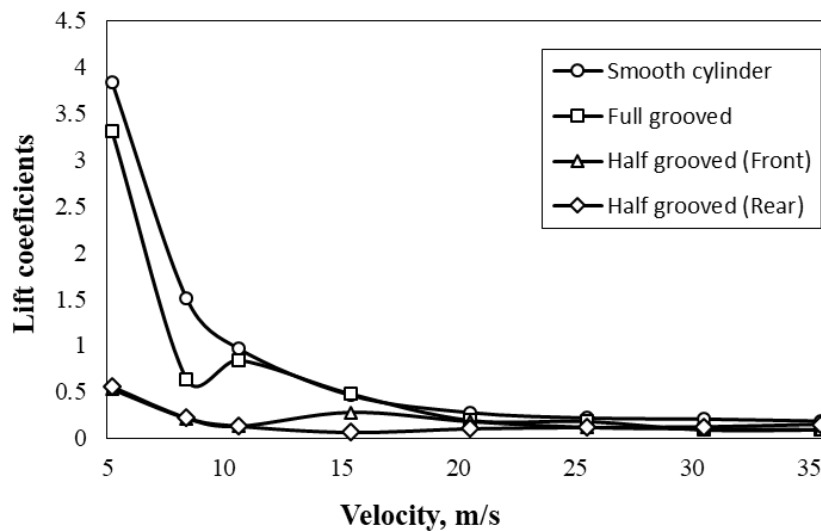


Fig. 7. Graphs of Lift Coefficient against velocity for all cylinders

### 3.3 Flow Visualization Test

Flow visualization, which is one of the objectives of this research, is used to analyze the flow separation and wake generation characteristics of each cylinder. Flow separation is related to drag coefficient on bluff bodies, such as a cylinder. A smoke visualization technique is used for the flow visualization test. A constant airspeed of 1.5m/s was set during the test. Flow patterns were observed and the separation points off the cylinders were determined. The length of the recirculation zone was measured from the front end of the cylinder (in the stream wise direction). Figure 8 shows the flow visualization results of the smooth, half grooved and full grooved cylinders at 1.5m/s.

From the results, it can be observed that the separation point of the smooth cylinder is located much closer to the front side of the cylinder than the half groove (rear), followed by half groove (front) and finally the full grooved cylinder. The recirculation length for the smooth cylinder was 96mm, and for the full grooved cylinder, 88mm. The recirculation length for the half grooved (front) cylinder measured 76mm, and for the half grooved (rear) cylinder was 99mm. The results obtained are in good agreement with those obtained by Zhou *et al.*, [18]; where grooved or dimpled cylinder resulted in shorter recirculation lengths than the smooth cylinder.

Traub *et al.*, [23] stated in their book that the increase in surface roughness reduced the drag coefficient by tripping the boundary layer into turbulence at a lower Reynold's number. Thus, delaying the flow separation, and causing the fluid to close behind the body; thus narrowing the wake and reducing the pressure drag considerably. Therefore, surfaces with higher surface roughness lead to lower recirculation lengths. The smoke visualization test results parallel the drag coefficient (CD) test; where the smallest drag coefficients are produced by the full grooved cylinder. In conclusion, the grooved surfaces are efficient at producing smaller wakes than the smooth cylinder. Grooved cylinders are also affective in delaying the separation that results in a smaller drag coefficient.

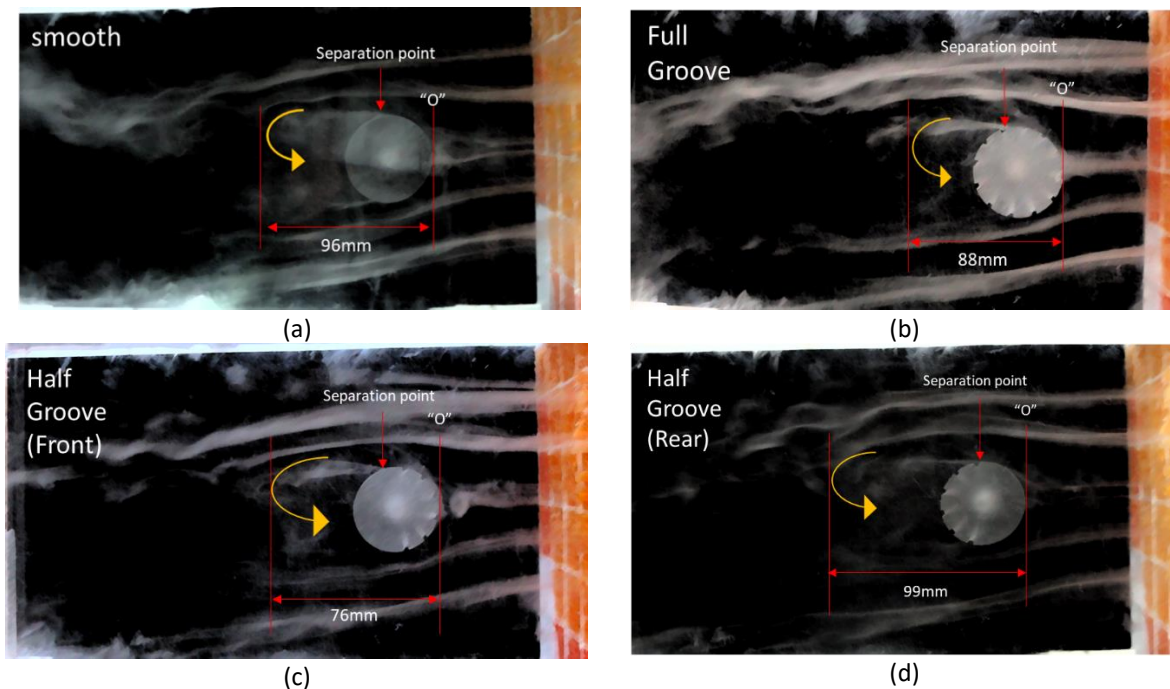


**Fig. 8.** Flow visualization results at 1.5m/s. (a) smooth cylinder (b) Full groove cylinder (c) Half groove (front) (d) Half groove (rear)

#### 4. Conclusions

The results indicate that groove-surfaced cylinders are effective in reducing drag, CD and lift CL coefficients; especially in the higher Reynold's number branch. The full grooved cylinder showed the highest reduction value, followed by the half groove located on the streamside, the half groove located on the leeside and finally, the smooth cylinder. This is consistent with the smoke visualization test results that the grooved surface roughness reduced the cylinder wake recirculation length. The smoke visualization test also indicates that the separation point on the grooved cylinder was further. Thus, resulting in a narrower wake size.

#### Acknowledgement

The authors would like to express their thanks to the RMC of UTM for the Research Grant, GUP (17H96,15J28,20H29), TDR Grant (05G23), FRGS Grant (5F074), School of Mechanical Engineering, UTM and Ministry of Higher Education for their support.

#### References

- [1] Butt, Usman, and Christoph Egbers. "Aerodynamic characteristics of flow over circular cylinders with patterned surface." *International Journal of Materials, Mechanics and Manufacturing* 1, no. 2 (2013): 121. <https://doi.org/10.7763/IJMMM.2013.V1.27>
- [2] Syahrullail, Samion, Jazair Yahya Wira, W. B. Wan Nik, and W. N. Fawwaz. "Friction characteristics of RBD palm olein using four-ball tribotester." In *Applied Mechanics and materials*, vol. 315, pp. 936-940. Trans Tech Publications Ltd, 2013. <https://doi.org/10.4028/www.scientific.net/AMM.315.936>
- [3] Razak, D. M., S. Syahrullail, N. Sapawe, Y. Azli, and N. Nuraliza. "A new approach using palm olein, palm kernel oil, and palm fatty acid distillate as alternative biolubricants: improving tribology in metal-on-metal contact." *Tribology Transactions* 58, no. 3 (2015): 511-517. <https://doi.org/10.1080/10402004.2014.989348>
- [4] Hassan, Mohammed, Farid Nasir Ani, and S. Syahrullail. "Tribological performance of refined, bleached and deodorised palm olein blends bio-lubricants." *Journal of Oil Palm Research* 28, no. 4 (2016): 510-519.



- <https://doi.org/10.21894/jopr.2016.2804.12>
- [5] Syahrullail, S., M. A. M. Hariz, MK Abdul Hamid, and A. A. Bakar. "Friction characteristic of mineral oil containing palm fatty acid distillate using four ball tribo-tester." *Procedia Engineering* 68 (2013): 166-171.  
<https://doi.org/10.1016/j.proeng.2013.12.163>
- [6] Golshokouh, Iman, S. Syahrullail, Farid Nasir Ani, and H. H. Masjuki. "Investigation of Palm Fatty Acid Distillate Oil as an Alternative to Petrochemical Based Lubricant." *Journal of Oil Palm Research* 26, no. 1 (2014): 25-36.
- [7] Bearman, P. W., and J. K. Harvey. "Control of circular cylinder flow by the use of dimples." *AIAA journal* 31, no. 10 (1993): 1753-1756.  
<https://doi.org/10.2514/3.11844>
- [8] Alam, Md Mahbub, M. Moriya, and H. Sakamoto. "Aerodynamic characteristics of two side-by-side circular cylinders and application of wavelet analysis on the switching phenomenon." *Journal of Fluids and Structures* 18, no. 3-4 (2003): 325-346.  
<https://doi.org/10.1016/j.jfluidstructs.2003.07.005>
- [9] Eppakayala Naresh, Pinnamaneni Dileep Kumar, B. Nagaraj Goudand Anil Kumar. N. "Drag Reduction over a Circular Cylinder." *International Journal of Civil Engineering and Technology* 88 no. 8 (2017): 1334-1345.
- [10] Doreti, Lalith Kumar, and L. Dineshkumar. "Control techniques in flow past a cylinder-A Review." In *IOP Conference Series: Materials Science and Engineering*, vol. 377, no. 1, p. 012144. IOP Publishing, 2018.  
<https://doi.org/10.1088/1757-899X/377/1/012144>
- [11] Achenbach, Elmar. "Influence of surface roughness on the cross-flow around a circular cylinder." *Journal of fluid mechanics* 46, no. 2 (1971): 321-335.  
<https://doi.org/10.1017/S0022112071000569>
- [12] Güven, Oktay, Cesar Farell, and V. C. Patel. "Surface-roughness effects on the mean flow past circular cylinders." *Journal of Fluid Mechanics* 98, no. 4 (1980): 673-701.  
<https://doi.org/10.1017/S0022112080000341>
- [13] Syahrullail, S., C. S. N. Azwadi, MR Abdul Kadir, and N. E. A. Shafie. "The effect of tool surface roughness in cold work extrusion." *Journal of Applied Science* 11 (2011): 367-372.  
<https://doi.org/10.3923/jas.2011.367.372>
- [14] Aoki, Katsumi, Atsuo Ohike, Kiyonaga Yamaguchi, and Yasuki Nakayama. "Flying characteristics and flow pattern of a sphere with dimples." *Journal of visualization* 6, no. 1 (2003): 67-76.
- [15] Muhammad Arif Dandan, Syahrullail Samion, Mohamad Nor Musa, and Fazila M. Zawawi. "Evaluation of Lift and Drag Force of Outward Dimple Cylinder Using Wind Tunnel." *CFD Letters* 11, no. 3 (2019): 145-153.
- [16] Kimura, Takeyoshi, and Michihisa Tsutahara. "Fluid dynamic effects of grooves on circular cylinder surface." *AIAA journal* 29, no. 12 (1991): 2062-2068.  
<https://doi.org/10.2514/3.10842>
- [17] Song, Xiaowen, Yuchen Qi, Mingxiao Zhang, Guogeng Zhang, and Wenchao Zhan. "Application and optimization of drag reduction characteristics on the flow around a partial grooved cylinder by using the response surface method." *Engineering Applications of Computational Fluid Mechanics* 13, no. 1 (2019): 158-176.  
<https://doi.org/10.1080/19942060.2018.1562382>
- [18] Zhou, Bo, Xikun Wang, Wei Guo, Jiabin Zheng, and Soon Keat Tan. "Experimental measurements of the drag force and the near-wake flow patterns of a longitudinally grooved cylinder." *Journal of Wind Engineering and Industrial Aerodynamics* 145 (2015): 30-41.  
<https://doi.org/10.1016/j.jweia.2015.05.013>
- [19] Lo, K. W., and N. W. M. Ko. "Vortex interaction in the formation region of a grooved circular cylinder." *Fluid dynamics research* 24, no. 3 (1999): 161.  
[https://doi.org/10.1016/S0169-5983\(98\)00023-9](https://doi.org/10.1016/S0169-5983(98)00023-9)
- [20] Guangyao, C. U. I., P. A. N. Chong, W. U. Di, Y. E. Qingqing, and W. A. N. G. Jinjun. "Effect of drag reducing riblet surface on coherent structure in turbulent boundary layer." *Chinese Journal of Aeronautics* 32, no. 11 (2019): 2433-2442.  
<https://doi.org/10.1016/j.cja.2019.04.023>
- [21] Cheng, W., D. I. Pullin, and Ravi Samtaney. "Large-eddy simulation of flow over a rotating cylinder: the lift crisis at  $Re_D = 6 \times 10^4$ ." *Journal of Fluid Mechanics* 855 (2018): 371-407.  
<https://doi.org/10.1017/jfm.2018.644>
- [22] Salam, Md Abdus, Vikram Deshpande, Nafiz Ahmed Khan, and MA Taher Ali. "Numerical Analysis of Effect of Leading-Edge Rotating Cylinder on NACA0021 Symmetric Airfoil." *European Journal of Engineering Research and Science* 4, no. 7 (2019): 11-17.  
<https://doi.org/10.24018/ejers.2019.4.7.1385>

- 
- [23] Traub, Lance W., Anthony Munson, and Justin McBurney. "Experimental study of drag reduction on a golf driver club using discrete surface elements." *Sports Engineering* 22, no. 2 (2019): 12.  
<https://doi.org/10.1007/s12283-019-0305-6>